Journal of Controlled Release 140 (2009) 34–39

Contents lists available at ScienceDirect

Journal of Controlled Release

journal homepage: www.elsevier.com/locate/jconrel

Influence of surface chemistry of mesoporous alumina with wide pore distribution on controlled drug release

Shobhna Kapoor, Rajesh Hegde, Aninda J. Bhattacharyya *

Solid State and Structural Chemistry Unit, Indian Institute of Science, Bangalore 560012, India

ARTICLE INFO

Article history:
Received 18 May 2009
Accepted 28 July 2009
Available online 3 August 2009

Keywords:
Controlled drug delivery
Mesoporous alumina
Surface chemistry
Pore morphology

ABSTRACT

The crucial role of the drug carrier surface chemical moeities on the uptake and *in vitro* release of drug is discussed here in a systematic manner. Mesoporous alumina with a wide pore size distribution (2–7 nm) functionalized with various hydrophilic and hydrophobic surface chemical groups was employed as the carrier for delivery of the model drug ibuprofen. Surface functionalization with hydrophobic groups resulted in low degree of drug loading (approximately 20%) and fast rate of release (85% over a period of 5 h) whereas hydrophilic groups resulted in a significantly higher drug payloads (21%–45%) and slower rate of release (12%–40% over a period of 5 h). Depending on the chemical moiety, the diffusion controlled ($\propto \text{time}^{-0.5}$) drug release was additionally observed to be dependent on the mode of arrangement of the functional groups on the alumina surface as well as on the pore characteristics of the matrix. For all mesoporous alumina systems the drug dosages were far lower than the maximum recommended therapeutic dosages (MRTD) for oral delivery. We envisage that the present study would aid in the design of delivery systems capable of sustained release of multiple drugs.

1. Introduction

Inorganic nanostructured oxide materials have found widespread application as controlled drug delivery systems (DDS) [1–8]. The most important advantage of inorganic nanostructured materials as DDS is that their structures are able to resist degradation and hence facilitate release of drugs at requisite times and in requisite amounts unlike other forms of DDS such as liposomes or polymers which degrade prematurely lead to poor yields at the target site. Mesoporous material such as MCM-41 (Mobil Crystalline Materials — MCM) was demonstrated as DDS for the first time in 2001 by the group of Vallet-Regi et al. [4]. Since then considerable efforts have been devoted in synthesizing mesoporous materials (Michigan State University — MSU; Hollow/Hexagonal Mesoporous Silica — HMS) for use as DDS. Mesoporous materials offer several attractive features such as (a) stable porous structure (b) large surface area [9] (c) tunable pore sizes and volumes and (d) easier chemical functionalization of the surface [10]. All these features aid in better manipulation of drug loading and release. These intrinsic features also make mesoporous materials versatile hosts for variety of biomacromolecules such as proteins [11,12].

It has been shown that the most effective way to control release profile of a drug from mesoporous materials is to optimize drug–surface interaction via the suitable surface chemical functionalization. For example, when MCM-41/SBA (Santa Barbara Amorphous materials) [13] are functionalized with amino groups, the ionic interaction between the carboxyl groups on ibuprofen and amino groups on matrix leads to a slower release of drug in comparison to the rate of release from the non-functionalized material with surface hydroxyl groups. Another possibility for controlled release from mesoporous materials is through functionalization with hydrophobic species [14]. In this case the drug transport out of the matrix is affected as the aqueous medium is unable to penetrate through the pores. Majority of the published literature on mesoporous oxide DDS are based on silica with pores of single size ~2.5 nm. In this paper, we discuss the prospect of a mesoporous oxide system having pores of varying sizes and different surface chemical functionalities as DDS. This allows studying the effect of surface functionality and pore size on drug loading and release using one single matrix and eliminating the need for synthesizing different matrices with different pore sizes. To suffice our purpose, commercially available mesoporous alumina with a wide intrinsic pore size distribution was selected as DDS for the study [3]. The influence of various surface chemical groups on drug ibuprofen uptake and release were systematically studied using X-ray diffraction, thermogravimetric analysis, Fourier transform infrared spectroscopy and time-dependent UV–VIS spectroscopy.

2. Materials and methods

2.1. Modification of Al_2O_3–OH with aminopropyltrimethoxysilane (APTMS) and methyltrimethoxysilane (MTMS)

Calculated amount of as received Al_2O_3–OH (200 mg) having surface hydroxyl groups [number density of OH groups ~12.5 nm^{-2}]

* Corresponding author. Fax: +91 80 23601310.
E-mail address: aninda_jb@sscu.iisc.ernet.in (A.J. Bhattacharyya).

0168-3659/$ – see front matter © 2009 Elsevier B.V. All rights reserved.
doi:10.1016/j.jconrel.2009.07.015

was added to 10 ml of toluene and stirred. 1 ml of the functionalizing moiety i.e. either 3-aminotrimethoxysilane or methylmethoxysilane respectively was added drop-wise slowly into the stirred solution. The solution was aged for 24 h and then washed with extra amount of toluene. After drying, the anchoring and amount of the functionalized group on the alumina surface was confirmed respectively by Fourier transform infrared spectroscopy (FTIR) and thermogravimetric analysis (TGA).

2.2. Modification of Al_2O_3–OH with 2,3-dihydroxynaphthalene (DN)

Commercially available DN in the amount of 460 mg was dissolved in 5 ml of acetone and stirred continuously. 230 mg of as received Al_2O_3–OH was added to the dihydroxynaphthalene–acetone solution and the solution mixture was aged overnight while stirring. The next stage involved the evaporation of the acetone at 95 °C. The resulting solid mixture of DN and Al_2O_3 was heated under N_2 flow at 300 °C for 1 h. At this step, dehydration occurs by the reaction between the hydroxyl groups of Al_2O_3 and hydroxyl groups of DN. The unreacted DN was removed by centrifuging the solution with acetone for 1 min. Finally, the mixture was dried to remove acetone.

2.3. Preparation of Al_2O_3–X (X = OH, NH_2, CH_3 and DN):IBU composite

Unmodified and modified mesoporous alumina was added to IBU–hexane solution yielding a mixture of Al_2O_3 (in mg) to IBU–hexane solution (in ml) ratio of 120 mg mL^{-1}. Despite certain adverse effects, hexane has been the solvent of choice for several research groups working with inorganic nanostructured materials for prospective drug delivery applications. In a recent report [3] the utility of hexane as a solvent for loading drugs inside mesoporous oxides has been explicitly demonstrated by the group of Bhattacharyya at Bangalore. Among various solvents (including water) employed for preparation of drug–oxide composites, hexane was the best from the point of view of degree of drug solubility (40 mg mL^{-1}), degree of impregnation of the mesoporous matrix by the drug and duration for preparation of the drug–oxide composite. The procedure for loading ibuprofen into various Al_2O_3–X is as follows. The glass tube containing the Al_2O_3–X:IBU liquid solution mixture was completely dipped inside a Dewar flask containing liquid nitrogen and evacuated for 2 h for the complete removal of air from the pores. Following evacuation, the mixture was taken out from the Dewar flask and defrosted under vacuum at room temperature for 30 min. The oxide particles impregnated with drug in hexane was then ultrasonicated for few minutes. Finally, the mixture was dried at 55 °C for over a day for the complete removal of hexane. The dried composite samples are designated as Al_2O_3–X(X = OH, NH_2, CH_3, and DN):IBU.

2.4. Characterization experiments for studying degree of surface coverage by various functional groups and percentage of ibuprofen uptake inside Al_2O_3

The degree of drug loading in the oxide was studied using thermogravimetric analysis (TGA), X-ray diffraction (XRD), Fourier transform infrared (FTIR) spectroscopy and nitrogen adsorption/desorption. The TGA (Perkin Elmer Pyris6000) experiments were done by heating the sample in a silica crucible under nitrogen from room temperature (25 °C to 750 °C) at a heating rate of 10 °C min^{-1}. Wide-angle XRD (Phillips X'Pert Pro diffractometer, Cu-K_α radiation, $\lambda = 1.5418$ Å) data at 25 °C over the range $5° \leq 2\theta \leq 40°$ with step width and scan rate of 0.02° and 0.6° per min respectively was collected using a multipurpose sample holder. For the room temperature FTIR (Perkin Elmer FTIR Spectrometer Spectrum 1000) measurements, requisite amount of sample was mixed with pure spectroscopic grade potassium bromide (KBr) and was cast into pellet of diameter 1.3 cm and thickness ~0.1 cm. For the N_2 adsorption/desorption (Belsorp) experiments mesoporous Al_2O_3–X samples were degassed at 200 °C for 5 h whereas the oxide–drug composites were degassed at 30 °C for 5 h. CHN microanalysis (Perkin Elmer, 2400 CHNSO system) was done to estimate the grafting density of the various functional groups anchored on the alumina surface.

2.5. In vitro ibuprofen release kinetics

The *in vitro* drug release experiments were carried out by immersing the drug impregnated oxide samples into simulated body fluid (SBF) of pH 7.3, having a concentration of 3.33 mg of Al_2O_3–X:IBU per ml of SBF. SBF of pH = 7.3 was prepared as per the prescription in Ref [15]. The SBF composition is as follows: 0.14 M (Na^+), 0.005 M (K^+), 0.0025 M (Ca^{2+}), 0.0015 M (Mg^{2+}), 0.15 M (Cl^-), 0.0042 M (HCO_3^-), 0.001 M (HPO_4^{2-}), and 0.0005 M (SO_4^{2-}). The pH of the SBF was varied by the addition of requisite amounts of standard 1 M aqueous solutions of NaOH (Merck) or HCl (Merck). Amount of IBU released as a function of time at 25 °C in SBF was determined by UV–VIS spectroscopy (Perkin Elmer, Lambda 35 UV Spectrometer) by monitoring the changes in the absorbance at wavelength of 264 nm at suitable intervals of time.

3. Results and discussion

3.1. Estimation of IBU uptake and functional group coverage from thermogravimetry and CHN analysis

Fig. 1 shows the results of thermogravimetric analysis of Al_2O_3–X (X = OH, NH_2, CH_3, DN):IBU composites. For the Al_2O_3–NH_2:IBU, Al_2O_3–DN:IBU, Al_2O_3–OH:IBU and Al_2O_3–CH_3:IBU the drug loadings were 45%, 29%, 21% and 19% respectively. The loading fractions in all cases were estimated from the ratio of weight loss between 200 and 725°C to total initial weight of the Al_2O_3–X:IBU. The weight loss due to organic group coating was 14%, 10% and 6% for Al_2O_3–DN, Al_2O_3–NH_2 and Al_2O_3–CH_3 respectively (inset Fig. 1). This weight loss is attributed not to only the fraction chemically bound to the alumina surface but also to those which are held physically. Functionalization with various chemical moieties resulted in the decrease of surface area. This is corroborated by the estimation of grafting density of the various functional groups on the alumina surface by elemental analysis normalized to surface area (BET surface area = 190 m^2 g^{-1}) of the as received Al_2O_3. Estimations were done assuming all organic moieties

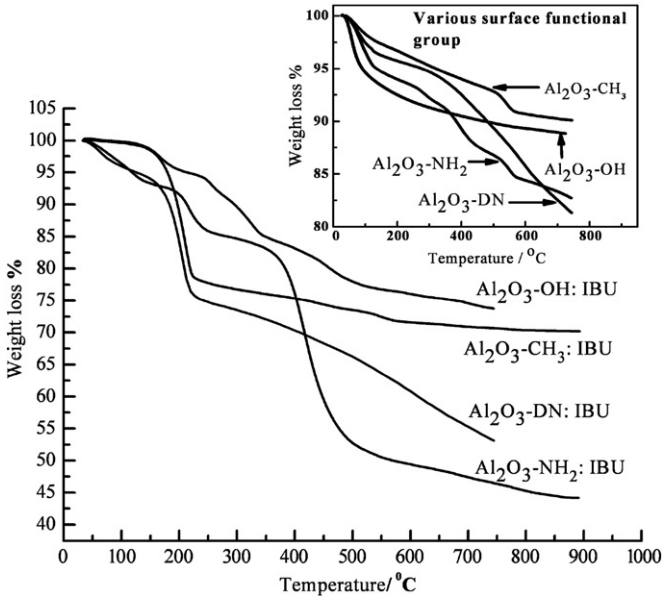

Fig. 1. Thermogravimetric analysis (TGA) of Al_2O_3–X:IBU. Temperature range: (25–750) °C, rate 10 °C min^{-1}. Inset: TGA for Al_2O_3–X.

being chemically bound to the oxide surface. The average density of OH groups on the alumina surface was taken to be 12.5 nm^{-2}. Estimations revealed approximately 80% coverage (grafting density = 10 nm^{-2}) for Al_2O_3–CH_3, while for Al_2O_3–NH_2 and Al_2O_3–DN it was approximately 55% (grafting density = 7 nm^{-2}) and 52% (grafting density = 6.5 nm^{-2}) respectively. Decrease in the BET surface area was also observed for Al_2O_3 following surface functionalization. This is discussed in the following section.

3.2. Estimation of surface area from N_2 adsorption/desorption studies

Impregnation of Al_2O_3–X (X = OH, NH_2, CH_3, DN) by IBU is also well supported by the N_2 adsorption/desorption isotherm. For all samples, the isotherms obtained are as depicted in Fig. 2 which resemble the standard type IV isotherm. The BET surface area for bare Al_2O_3–OH was calculated to be approximately 190 $m^2\ g^{-1}$. Surface functionalization of the mesoporous alumina resulted in a decrease in the surface area. The surface area of Al_2O_3–CH_3 was at minimum 77.7 $m^2\ g^{-1}$ (maximum surface coverage 80%). For Al_2O_3–NH_2 and Al_2O_3–DN the areas obtained were 95 $m^2\ g^{-1}$ and 115 $m^2\ g^{-1}$ respectively in accordance with the extent of surface coverage obtained from CHN estimates. For Al_2O_3–X:IBU composite samples, a drastic decrease in N_2 uptake and BET surface area was observed. The surface area for all Al_2O_3–X:IBU was found to be approximately 4 $m^2\ g^{-1}$.

3.3. Evidence of impregnation of Al_2O_3–X (X = OH, NH_2, CH_3, DN) by IBU using X-ray diffraction (XRD) studies

Fig. 3 shows the XRD patterns of Al_2O_3–X (X = OH, NH_2, CH_3, and DN) and Al_2O_3–X:IBU. XRD for Al_2O_3–X (X = OH, NH_2, CH_3, DN) is amorphous. Lack of periodicity [3] and dispersion in pore size may be probable reasons for the lack of appearance of any diffraction peak in XRD profiles. For Al_2O_3–X (X = OH, DN):IBU, peaks at $2\theta = 6.1°$, 12.3°, 16.7°, 17.7°, 18.8°, 19.2°, 19.6°, 20.2°, 22.4°, and 24.6° are attributed to those of pure IBU (Fig. 3 inset). The IBU peaks were less intense and broader compared to that observed in free IBU. Probable source for disorder in encapsulated IBU is due to the π–π interaction of IBU with benzene rings on Al_2O_3–DN. This results in smaller crystallites in case of encapsulated IBU compared to free IBU. The change in crystallite size is evident from analysis (Scherer formula) of the representative peak at $2\theta = 6.1°$. The IBU crystallite size changed from 1.5 nm for free IBU to 1.4 nm for Al_2O_3–DN:IBU to 0.3 nm for Al_2O_3–OH:IBU. Smaller crystallite size in case of Al_2O_3–OH:IBU compared to Al_2O_3–DN:IBU suggests stronger interaction between OH and IBU than between DN and IBU. Further support for enhanced disorder is via the observation of less intense peaks for Al_2O_3–OH:IBU and Al_2O_3–DN:IBU compared to that for free IBU. Apart from the chemical interaction, the higher intensity for Al_2O_3–DN:IBU than Al_2O_3–OH:IBU is also due to higher IBU uptake in case of Al_2O_3–DN than Al_2O_3–OH. The peak intensities in the X-ray diffraction profile for Al_2O_3–CH_3 are lower than that of Al_2O_3–DN but still higher compared to Al_2O_3–OH. The observation of retention of higher crystallinity in Al_2O_3–CH_3 compared to Al_2O_3–OH is attributed to the strength of interaction between the surface chemical entity and IBU. As the interaction between CH_3 and IBU is weaker than that between OH and IBU, IBU disordering is lower in case of CH_3 than OH. (Crystallite size estimated for Al_2O_3–CH_3:IBU was 1.8 nm compared to 0.3 nm for Al_2O_3–OH:IBU). It is also perceived that the higher intensity in case of Al_2O_3–DN and Al_2O_3–CH_3 may be due to certain fraction of IBU residing outside the pores in the free space between alumina particle aggregates. The residence of IBU outside the mesopores may also be as a result of the hydrophobicity of CH_3 and DN. In contrast, diffraction profile of Al_2O_3–NH_2:IBU show no peaks in spite having the highest drug uptake (45% as per TGA). Absence of IBU peaks in Al_2O_3–NH_2:IBU is attributed to the strong ionic interactions between IBU and surface NH_2 group leading to higher disordering of encapsulated IBU.

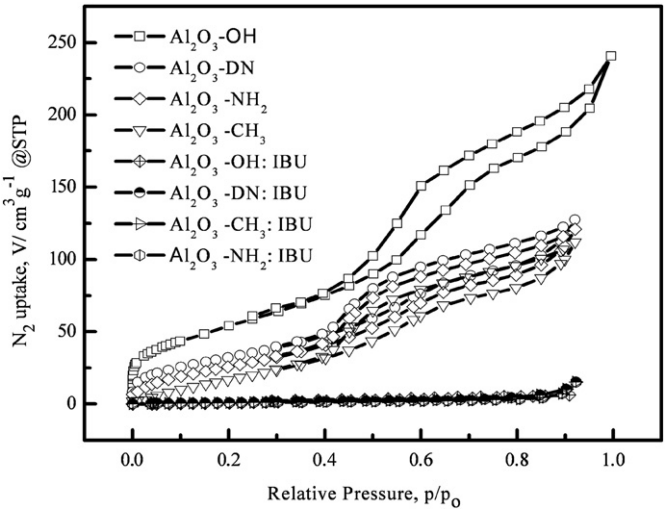

Fig. 2. N_2 adsorption/desorption isotherms for Al_2O_3–X and Al_2O_3–X:IBU.

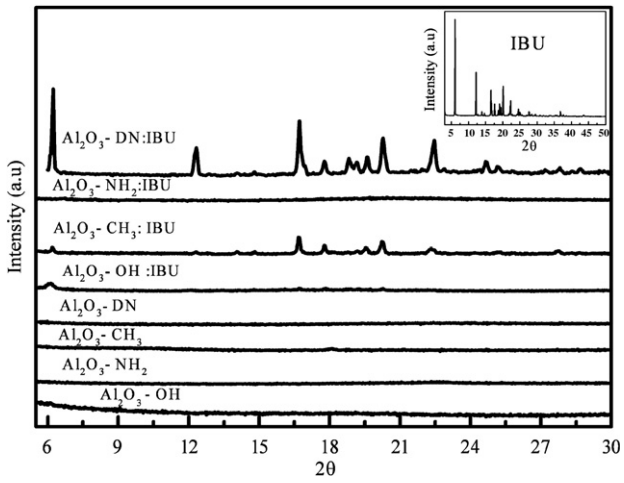

Fig. 3. X-ray diffraction (XRD) pattern at 25 °C for various Al_2O_3–X and Al_2O_3–X:IBU samples. Inset: XRD pattern for pure IBU.

3.4. Fourier transform infrared (FTIR) spectroscopy

Fig. 4 shows the Fourier transform infrared spectra for Al_2O_3–X, Al_2O_3–X:IBU and IBU. The peak in the range of 3750–3000 cm^{-1} is due to the Al–OH stretching frequency. For Al_2O_3–DN the OH stretch band almost diminishes upon functionalization with DN suggesting that all the Al–OH groups on the Al_2O_3–OH have reacted with DN. Surface functionalization with DN also results in the appearance of several new bands. Bands at 1460 cm^{-1} and 754 cm^{-1} are attributed respectively to C=C stretching vibrations and C–H out of plane deformation. Functionalization of Al_2O_3–OH surface with APTMS and MTMS also leads to the development of new bands. As shown in Fig. 4 bands for Al_2O_3–CH_3 are observed at 2971 cm^{-1} and 2854 cm^{-1} due to asymmetric and symmetric C–H stretchings respectively. For Al_2O_3–NH_2 bands observed at 1568 cm^{-1} and 1330 cm^{-1} are due to N–H bending and N–C stretching respectively. Bands at 3400 cm^{-1} and 3500 cm^{-1} are attributed to free symmetric and asymmetric N–H stretching modes. However, these vibrations modes are not deconvoluted from the Al–OH stretching frequency. Incorporation of IBU reduces the OH stretch band drastically suggesting a possible interaction between IBU and Al_2O_3–OH. This is further supported by the observation of decrease in COOH stretch band at 1719 cm^{-1}. The reduction is highest for Al_2O_3–NH_2:IBU

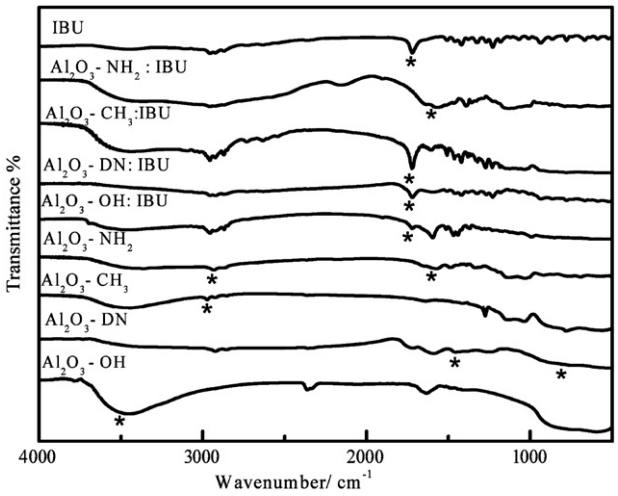

Fig. 4. Fourier transform infrared (FTIR) spectra at 25 °C for Al_2O_3–X, Al_2O_3–X:IBU and IBU.

compared to Al_2O_3–OH:IBU, Al_2O_3–CH_3:IBU and Al_2O_3–DN:IBU. Al_2O_3–NH_2:IBU composite shows the strongest interaction as the NH_2 group is the strongest base of all the chemical moieties used for the study. For Al_2O_3–DN:IBU the COOH band intensity is slightly higher than that of Al_2O_3–OH:IBU which suggests weaker interaction between the surface DN and IBU. However, the COOH band intensity is lower for Al_2O_3–DN:IBU lesser compared to Al_2O_3–CH_3:IBU. This is attributed to relatively stronger π–π interactions between DN and IBU compared to weaker hydrophobic interactions as in the case of Al_2O_3–CH_3:IBU. Evidence in support of the IBU interactions with modified Al_2O_3 can also be observed from the appearance of the COO^- asymmetric stretch band at approximately 1600 cm^{-1}. The intensity of COO^- band is highest for Al_2O_3–NH_2:IBU compared to Al_2O_3–OH:IBU, Al_2O_3–DN:IBU and Al_2O_3–CH_3:IBU which also further supports our proposition of the observed changes in the band due to interaction between IBU and varying chemical moiety on the alumina surface. Based on FTIR and XRD the strength of interaction between alumina surface and IBU can be summarized as follows Al_2O_3–NH_2 > Al_2O_3–OH > Al_2O_3–DN > Al_2O_3–CH_3.

3.5. In vitro ibuprofen release kinetics using time-dependent UV–VIS spectroscopy

Fig. 5 shows the *in vitro* release profile of ibuprofen at 25 °C from Al_2O_3(X = OH, NH_2, CH_3, DN):IBU into the simulated body fluid (SBF) (3.33 mg of Al_2O_3–X:IBU per ml of SBF [3]) at pH = 7.3. The

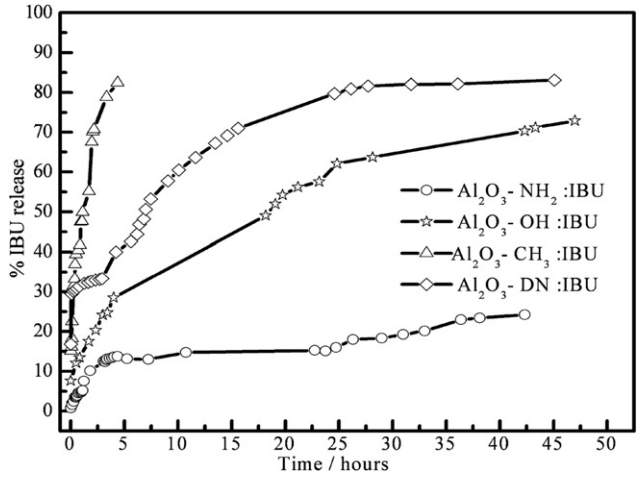

Fig. 5. Kinetic profile of IBU from Al_2O_3–X into SBF (pH = 7.0) at 25 °C.

concentration of IBU released in SBF as a function of time was determined by UV–VIS spectroscopy by monitoring the changes in absorbance at wavelength of 264 nm at suitable intervals of time. As discussed in previous sections, the strength of interaction between the alumina surface and IBU depends on the chemical moiety decorating the Al_2O_3 surface. The kinetic release profile of IBU from the Al_2O_3–X:IBU composites follows the same trend with the composite showing the strongest interaction between IBU and oxide surface results in slowest rate of release. Al_2O_3–CH_3:IBU shows the fastest rate of release with almost 85% of the drug molecules released in approximately 5 h. This is similar to oral drug delivery where the concentration of the drug increases within a very short period of time interval reaching concentrations higher than the maximum dosages as per the therapeutic window of the drug. As a consequence of the release profile the Al_2O_3–CH_3:IBU cannot be termed as a controlled drug delivery carrier. We suppose that a carrier such as Al_2O_3–CH_3 would be more suited for situations where a drug or one among multiple drugs is required in large concentrations within a short span of time. Al_2O_3–CH_3:IBU being predominantly hydrophobic in nature results in the weakest interaction between oxide surface and IBU. Moreover, as the CH_3 group is smaller in size compared with other functional groups used, it possesses the minimum steric hindrance. The formation of a polymeric organosilane network on the alumina surface (Fig. 6a) further increases the hydrophobic character of Al_2O_3–CH_3. As a consequence of this, the drug is very weakly held in the pore and when suspended in SBF, IBU molecules diffuse out rapidly showing the fastest release. For Al_2O_3–DN:IBU, 70% of the drug was released in the first 15 h (40% in 5 h) followed by saturation at about 80% in 45 h. The release is slower than that of Al_2O_3–CH_3:IBU but faster than Al_2O_3–NH_2:IBU and Al_2O_3–OH:IBU. This can again be explained in terms of the strength of interaction. The slow release in case of Al_2O_3–DN:IBU in comparison to Al_2O_3–CH_3:IBU is attributed to the dominance of attractive interaction (such as π–π) between the surface naphthalene group and IBU. Significant amount of IBU release takes place only when sufficient amount of solvent molecules have diffused through the channels of the mesoporous alumina for solvation of the drug. As seen in Fig. 6b the DN groups being larger in size compared to methyl show higher steric hindrance to the formation of a polymeric network. The hydrophobicity in case of Al_2O_3–DN is expected to be lower compared to that of Al_2O_3–CH_3. Al_2O_3–OH:IBU releases 40% of IBU in approximately 15 h (30% in 5 h) and then increases until it saturates at 70% in 40 h. As expected the release is even slower than Al_2O_3–CH_3:IBU and Al_2O_3–DN:IBU respectively due to stronger interaction between the OH groups on alumina and COOH on IBU. The release of only 70% IBU in almost 2 days suggests probable retention of IBU inside the smaller pores of alumina (pore sizes ≤ 2 nm). The diffusion of solvent into the small pores and the counter diffusion of IBU out of the channels are severely restricted leading to delayed delivery of the drug. Finally, Al_2O_3–NH_2:IBU releases only 14% in 15 h and then saturates at about 23% in 40 h. As discussed in the previous section the slow release rate is attributed to the strong interaction between the NH_2 group of the ATPMS and COO^- of IBU. As NH_2 is a stronger base than OH the interaction is stronger resulting in a very slow rate of release rate of IBU from Al_2O_3–NH_2:IBU. Moreover, as the propyl chains in APTMS are longer than the methyl chain of MTMS, the steric hindrance needed to be overcome for the formation of a polymeric organosilane network is also quite large. This leads to monolayer formation on the alumina surface (Fig. 6c). As previously mentioned while the strength of the interaction between the alumina surface and IBU follows the order as Al_2O_3–NH_2 > Al_2O_3–OH > Al_2O_3–DN > Al_2O_3–CH_3, the release rates of the Al_2O_3–X:IBU composites follow the opposite trend with Al_2O_3–NH_2 < Al_2O_3–OH < Al_2O_3–DN < Al_2O_3–CH_3. In case of Al_2O_3–OH and Al_2O_3–NH_2 it is observed that in addition to the strength of the interaction of IBU with the oxide surface chemical moieties, the mesopore morphology such as pore size has also to be taken into

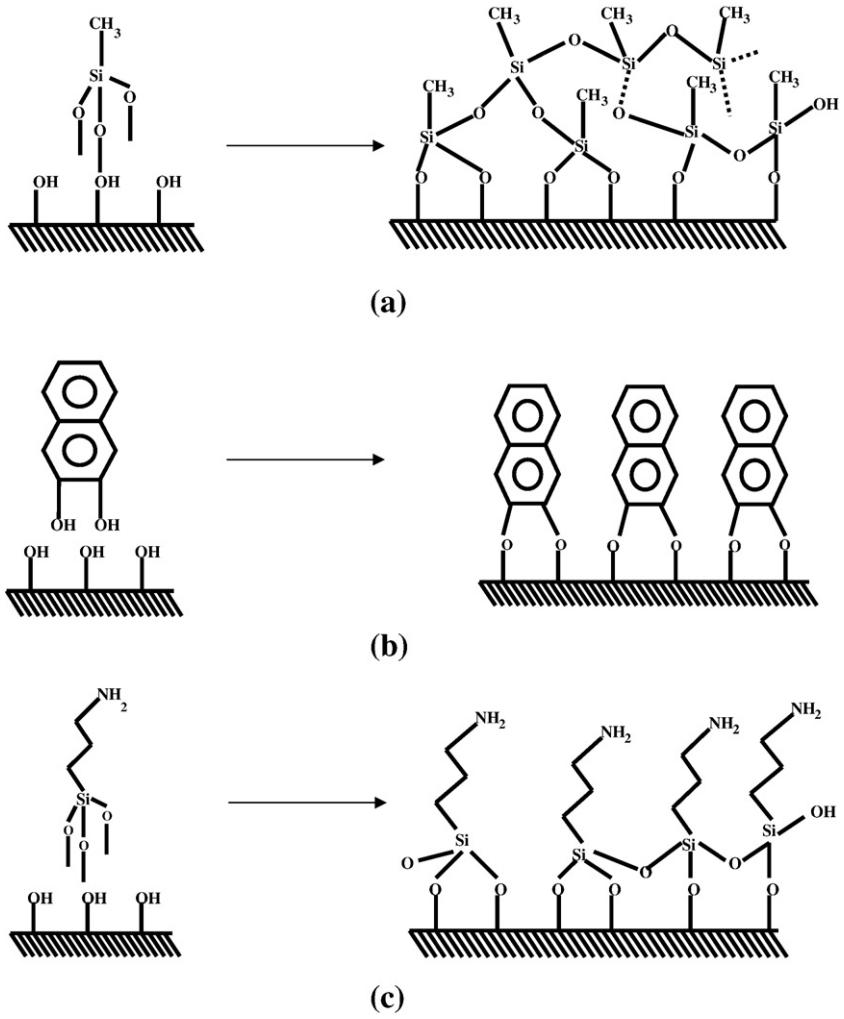

Fig. 6. (a) Polymeric organosilane network formed by the MTMS functional groups imparting high degree of hydrophobicity to the surface. (b) Monolayer coverage by DN groups imparting intermediate degree of hydrophobicity to the surface. (c) Monolayer coverage by APTMS functional group imparting hydrophilic nature to the surface.

account for the interpretation of drug release kinetics. Linear relationship between the amount of IBU released, [IBU] versus square root of time suggests a diffusion process for all Al_2O_3–X:IBU composites. For Al_2O_3–CH_3:IBU; $[IBU] = 39.4t^{0.5}$, Al_2O_3–DN:IBU; $[IBU] = 10.84t^{0.5}$, for Al_2O_3–NH_2:IBU; $[IBU] = 3.6t^{0.5}$, and Al_2O_3–OH:IBU; $[IBU] = 10.3t^{0.5}$. The efficiency of a drug delivery system is determined by the residence time of drug concentrations within therapeutic window for a particular drug. In the present study considering the drug release yields over a period of 24 h, Al_2O_3–CH_3:IBU results in a higher dosage of IBU (0.038 mg/kg-bw/day; bw: body weight taken as 60 kg) comparable to oral drug delivery whereas Al_2O_3–NH_2:IBU would result in a lowest dosage of 0.0115 mg/kg-bw/day. The dosages for Al_2O_3–DN:IBU and Al_2O_3–OH:IBU were found to be intermediate and are respectively 0.033 mg/kg-bw/day and 0.0201 mg/kg-bw/day. As no numerical estimates for drug dosages using controlled drug delivery systems are available it is not possible at his juncture to judge the extent of clinical utility of Al_2O_3–X:IBU controlled drug delivery systems. However the dosages for Al_2O_3–X:IBU were found to be much lower in comparison to the maximum recommended therapeutic dosages (MRTD) for oral delivery (~40 mg/kg-bw/day) [16].

4. Conclusions

We have demonstrated here in a convincing manner the importance of DDS surface chemistry on the uptake and release of small therapeutic molecule such as ibuprofen. Our results show that drug load and rate of release are heavily dependent on the type and concentration of the chemical groups present on the drug carrier surface. These determine to a great extent the strength of the interaction between the drug and surface chemical moiety. In addition depending on the surface chemical moiety, the rate of release was also found to be dependent on their mode of arrangement on the drug carrier surface as well as on the matrix pore morphology. Our findings reveal that drug carriers with hydrophobic chemical moiety on the surface show faster rates of drug release. We believe that the parameters of the buffer solution such as pH might also influence release kinetics [3]. We wish to report such studies in the near future. In the light of our results presented here it would be worthwhile to synthesize nanostructured materials with surfaces decorated with both hydrophobic and hydrophilic groups such as “Janus particles” [17,18]. Presence of varied chemical moieties on the surface of a single drug carrier would also be highly beneficial for tuning payloads and rate of release of more than one type of drug. However, in case of multiple drugs the morphology of the porous inorganic nanostructured material needs due consideration for maximization of benefits. For delivery of multiple drugs, we prescribe matrices with varying pore size distribution similar to the mesoporous alumina system used in the present study to be more appropriate than mesoporous systems with pores of single size such as MCM-silica. The influence of surface chemistry on the function of nanostructured material as exemplified here for the field of pharmaceutics is also of tremendous importance

in other fields such as catalysis and ionics [19]. We expect that suitable engineering of surfaces of inorganic nanostructured materials will lead to several interesting and multifunctional materials.

Acknowledgements

The authors thank I.S. Jarali for BET, TGA, FTIR, A. Mondal (Institute of Nanoscience Initiative, IISc. Bangalore) for TEM. We also thank Shyamal K. Das and Soumit S. Mandal, SSCU, IISc., Bangalore for useful discussions.

Appendix A. Supplementary data

Supplementary data associated with this article can be found, in the online version, at doi:10.1016/j.jconrel.2009.07.015.

References

[1] M. Hartmann, Ordered mesoporous materials for bioadsorption and biocatalysis, Chem. Mater. 17 (2005) 4577–4593.
[2] I.I Slowing, B.G. Trewyn, V.S.-Y. Lin, Mesoporous silica nanoparticles for intracellular delivery of membrane-impermeable proteins, J. Am. Chem. Soc. 129 (2007) 8845–8849.
[3] S.K. Das, S. Kapoor, H. Yamada, A.J. Bhattacharyya, Effects of surface acidity and pore size of mesoporous alumina on degree of loading and controlled release of ibuprofen, Mesopor. Micropor. Mater. 118 (2009) 267–272.
[4] M. Vallet-Regi, A. Ramila, R.P. del Real, J. Perez-Pariente, A new property of MCM-41: drug delivery system, Chem. Mater. 13 (2001) 308–311.
[5] J.M. Rosenholm, M. Lindén, Towards establishing structure–activity relationships for mesoporous silica in drug delivery applications, J. Control. Release 128 (2008) 157–164.
[6] A. Bernardos, E. Aznar, C. Coll, R. Martínez-Mañez, J.M. Barat, M.D. Marcos, F. Sancenón, A. Benito, J. Soto, Controlled release of vitamin B_2 using mesoporous materials functionalized with amine-bearing gate-like scaffoldings, J. Control. Release 131 (2008) 181–189.
[7] M. Bikram, A.M. Gobin, R.E. Whitmire, J.L. West, Temperature-sensitive hydrogels with SiO_2–Au nanoshells for controlled drug delivery, J. Control. Release 123 (2007) 219–227.
[8] A. Tan, S. Simovic, A.K. Davey, T. Rades, C.A. Prestidge, Silica-lipid hybrid (SLH) microcapsules: a novel oral delivery system for poorly soluble drugs, J. Control. Release 134 (2009) 62–70.
[9] J. Wang, A. Vinu, M.-O. Coppens, Synthesis and structure of silicalite-l/SBA-15 composites prepared by carbon templating and crystallization, J. Mater. Chem. 17 (2007) 4265–4273.
[10] A. Vinu, K.Z. Hossain, K. Ariga, Recent advances in functionalization of mesoporous silica, J. Nanosci. Nanotech. 5 (2005) 347–371.
[11] A. Vinu, C. Streb, V. Murugesan, M. Hartmann, Adsorption of cyctochrome C on new mesoporous carbon molecular sieves, J. Phys. Chem. B 107 (2003) 8297–8299.
[12] A. Vinu, M. Miyahara, K. Ariga, Biomaterial immobilization in nanoporous carbon molecular sieves: influence of solution pH, pore volume and pore diameter, J. Phys. Chem. B 109 (2005) 6436–6441.
[13] S.W. Song, K. Hidajat, S. Kawi, Functionalized SBA-15 materials as carriers for controlled drug delivery: influence of surface properties on matrix–drug interactions, Langmuir 21 (2005) 9568–9575.
[14] J.C. Doadrio, E.M.B. Sousa, I.I. Barba, A.L. Doadrio, J. Perez-Pariente, M. Vallet-Regi, Functionalization of mesoporous materials with long alkyl chains as a strategy for controlling drug delivery pattern, J. Mater.Chem. 16 (2006) 462–467.
[15] T. Kokubo, H. Kushitani, S. Sakka, T. Kitsugi, T. Yamamuro, Solutions able to reproduce in vivo surface-structure changes in bioactive glass-ceramic A_W^3, J. Biomed. Mater. Res. 24 (1990) 721–734.
[16] http://www.fda.gov/Cder/Offices/OPS_IO/MRTD.htm.
[17] A. Perro, S. Reculusa, F. Pereira, M.-H. Delville, C. Mingotaud, E. Duguet, E. Bourgeat- Lami, S. Ravaine, Towards large amounts of Janus nanoparticles through a protection— deprotection route, Chem. Comm. 44 (2005) 5542–5543.
[18] A. Perro, S. Reculusa, S. Ravaine, E. Bourgeat-Lami, E. Duguet, Design and synthesis of Janus micro- and nanoparticles, J. Mater. Chem. 15 (2005) 3745–3760.
[19] S.K. Das, A.J. Bhattacharyya, Oxide particle surface chemistry and ion transport in "soggy sand" electrolytes, J. Phys. Chem. C 113 (2009) 6699–6705.